Hadron Structure '15
International Journal of Modern Physics: Conference Series
Vol. 39 (2015) 1560112 (6 pages)

DOI: 10.1142/S201019451560112X

World Scientific
www.worldscientific.com

Physical observables in the decay $\Lambda_b \to \Lambda_c(\to \Lambda + \pi) + \tau^- + \bar{\nu}_\tau$

N. Habyl

Al-Farabi Kazakh National University
480012 Almaty, Kazakhstan
nuigui@mail.ru

Thomas Gutsche

Institut für Theoretische Physik, Universität Tübingen
D-72076, Tübingen, Germany

Mikhail A. Ivanov

BLTP, Joint Institute for Nuclear Research
141980 Dubna, Russia

Jürgen G. Körner

Institut für Physik, Johannes Gutenberg-Universität
D-55099 Mainz, Germany

Valery E. Lyubovitskij

Institut für Theoretische Physik
Universität Tübingen, Tübingen, Germany

Department of Physics, Tomsk State University
634050 Tomsk, Russia

Tomsk Polytechnic University, 634050 Tomsk, Russia

Pietro Santorelli

Università di Napoli Federico II, 80126 Napoli, Italy

INFN, Sezione di Napoli, 80126 Napoli, Italy

Published 26 November 2015

We analyze the tauonic semileptonic baryon decays $\Lambda_b^0 \to \Lambda_c^+ + \tau^- + \bar{\nu}_\tau$ with particular emphasis on the lepton helicity flip contributions which vanish for zero lepton masses. We calculate the total rate, differential decay distributions, the longitudinal and transverse polarization components of the Λ_c^+ and the τ^-, and the lepton-side forward-backward

asymmetries. We use the covariant confined quark model to provide numerical results on these observables.

Keywords: Relativistic quark model; light and heavy baryons; decay rates and asymmetries.

PACS Numbers: 12.39.Ki, 13.30.Eg, 14.20.Jn, 14.20.Mr

1. Motivation

Recently there has been much discussion about tensions and discrepancies of some of the experimental results on leptonic, semileptonic and rare decays involving (heavy) μ and τ leptons with the predictions of the Standard Model (SM). Among these are the tauonic B decays $B \to \tau\nu$, $B \to D\,\tau\bar{\nu}_\tau$ and $B \to D^*\,\tau\bar{\nu}_\tau$ and the muonic decays $B \to K^*\mu^+\mu^-$ and $\mathrm{Br}[B \to K\mu^+\mu^-]/\mathrm{Br}[B \to Ke^+e^-]$. The situation has been nicely summarized in Refs. 1–4.

This observation has inspired a number of searches for new physics beyond the SM (BSM) in charged current interactions. Details can be found in the recent literature on this subject (see, e.g. Refs. 5–17).

Motivated by the discrepancy between theory and experiment in the meson sector we have analyzed in Ref. 21 the corresponding semileptonic baryon decays $\Lambda_b^0 \to \Lambda_c^+ + \tau^- + \bar{\nu}_\tau$ within the SM with particular emphasis on the lepton helicity flip contributions which vanish for zero lepton masses. As in Refs. 18–20 we have described the semileptonic decays using the helicity formalism which allows one to include lepton mass and polarization effects without much additional effort. We have calculated the total rate, differential decay distributions, the longitudinal and transverse polarization of the daughter baryon and lepton-side forward-backward asymmetries.

Here, we give a brief sketch of the results obtained in Ref. 21 starting with the exact definition of physical observables via helicity amplitudes squared. Then we provide numerical results on these observables by using the covariant confined quark model. Also we replace an erroneous factor of "$-3/2$" with the correct factor of "$-3/4$" in the definition of the forward-backward asymmetry and provide correct numerical results for this quantity.

2. Helicity Amplitudes and the Polarization Observables

The matrix element of the process $\Lambda_b^0(p_1) \to \Lambda_c^+(p_2) + W^-_{\text{off-shell}}(q)$ is expressed via the vector and axial vector current matrix elements which can be expanded in terms of a complete set of invariants

$$M_\mu^V(\lambda_1,\lambda_2) = \bar{u}_2(p_2,\lambda_2)\left[F_1^V(q^2)\gamma_\mu - \frac{F_2^V(q^2)}{M_1}i\sigma_{\mu\nu}q^\nu + \frac{F_3^V(q^2)}{M_1}q_\mu\right]u_1(p_1,\lambda_1),$$

$$M_\mu^A(\lambda_1,\lambda_2) = \bar{u}_2(p_2,\lambda_2)\left[F_1^A(q^2)\gamma_\mu - \frac{F_2^A(q^2)}{M_1}i\sigma_{\mu\nu}q^\nu + \frac{F_3^A(q^2)}{M_1}q_\mu\right]\gamma_5 u_1(p_1,\lambda_1) \tag{1}$$

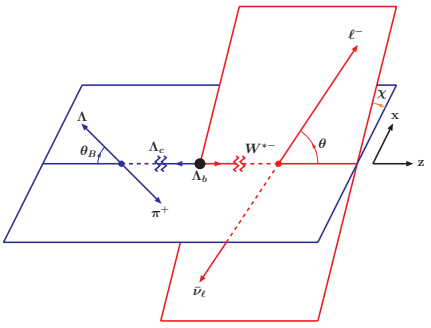

Fig. 1. Definition of the angles θ, θ^* and χ.

where $\sigma_{\mu\nu} = \frac{i}{2}(\gamma_\mu\gamma_\nu - \gamma_\nu\gamma_\mu)$ and $q = p_1 - p_2$. The labels $\lambda_i = \pm\frac{1}{2}$ denote the helicities of the two baryons.

It is easiest to calculate the helicity amplitudes in the rest frame of the parent baryon B_1 where we choose the z–axis to be along the $W^-_{\text{off-shell}}$ (see Fig. 1). They read[21]

$$\begin{aligned} H^{V/A}_{+\frac{1}{2}t} &= \frac{\sqrt{Q_+}}{\sqrt{q^2}}\left(M_- F_1^{V/A} \pm \frac{q^2}{M_1} F_3^{V/A}\right), \\ H^{V/A}_{+\frac{1}{2}+1} &= \sqrt{2Q_-}\left(F_1^{V/A} \pm \frac{M_+}{M_1} F_2^{V/A}\right), \\ H^{V/A}_{+\frac{1}{2}0} &= \frac{\sqrt{Q_-}}{\sqrt{q^2}}\left(M_+ F_1^{V/A} \pm \frac{q^2}{M_1} F_2^{V/A}\right), \end{aligned} \tag{2}$$

where we make use of the abbreviations $M_\pm = M_1 \pm M_2$ and $Q_\pm = M_\pm^2 - q^2$.

The physical observables can be expressed in terms of helicity structure functions given in terms of bilinear combinations of helicity amplitudes, see Table I of Ref. 21.

One obtains the normalized differential rate expressed in terms of the helicity structure functions

$$\begin{aligned} \frac{d\Gamma}{dq^2} &= \Gamma_0 \frac{(q^2 - m_\ell^2)^2 |\mathbf{p_2}|}{M_1^7 q^2}\{\mathcal{H}_U + \mathcal{H}_L + \delta_\ell[\mathcal{H}_U + \mathcal{H}_L + 3\mathcal{H}_S]\} \\ &\equiv \Gamma_0 \frac{(q^2 - m_\ell^2)^2 |\mathbf{p_2}|}{M_1^7 q^2}\mathcal{H}_{\text{tot}}. \end{aligned} \tag{3}$$

A forward-backward asymmetry is defined by

$$A^\ell_{FB}(q^2) = \frac{d\Gamma(F) - d\Gamma(B)}{d\Gamma(F) + d\Gamma(B)} = -\frac{3}{4}\frac{H_P + 4\delta_\ell H_{SL}}{H_{\text{tot}}}. \tag{4}$$

One defines a convexity parameter $C_F(q^2)$ according to

$$C_F(q^2) = \frac{3}{4}(1 - 2\delta_\ell)\frac{H_U - 2H_L}{H_{\text{tot}}}. \tag{5}$$

We obtain the $\cos\theta$ averaged polarization components of the daughter baryon B_2 ($B_2 = \Lambda_c^+$ in the present application). One obtains

$$P_z^h(q^2) = \frac{\rho_{1/2\,1/2} - \rho_{-1/2\,-1/2}}{\rho_{1/2\,1/2} + \rho_{-1/2\,-1/2}} = \frac{\mathcal{H}_P + \mathcal{H}_{L_P} + \delta_\ell\,(\mathcal{H}_P + \mathcal{H}_{L_P} + 3\mathcal{H}_{S_P})}{H_{\rm tot}},$$
$$P_x^h(q^2) = \frac{2\,{\rm Re}\,\rho_{1/2\,-1/2}}{\rho_{1/2\,1/2} + \rho_{-1/2\,-1/2}} = -\frac{3\pi}{4\sqrt{2}}\frac{\mathcal{H}_{LT} - 2\,\delta_\ell \mathcal{H}_{ST_P}}{\mathcal{H}_{\rm tot}}. \tag{6}$$

We have calculated the $\cos\theta$ averaged polarization components of the lepton with helicity flip contributions which can considerably change the magnitude of the polarization $|\vec{P}^\ell|$ and its orientation:

$$P_z^\ell(q^2) = -\frac{\mathcal{H}_U + \mathcal{H}_L - \delta_\ell(\mathcal{H}_U + \mathcal{H}_L + 3\mathcal{H}_S)}{\mathcal{H}_{\rm tot}},$$
$$P_x^\ell(q^2) = -\frac{3\pi}{4\sqrt{2}}\sqrt{\delta_\ell}\frac{\mathcal{H}_P - 2\mathcal{H}_{SL}}{\mathcal{H}_{\rm tot}}. \tag{7}$$

The polarization of the Λ_c^+ can be probed by analyzing the angular decay distribution of the subsequent decay of the Λ_c^+. One can exploit the cascade nature of the decay $\Lambda_b^0 \to \Lambda_c^+(\to \Lambda^0 + \pi^+) + W^-_{\text{off-shell}}(\to \ell^- + \bar{\nu}_\ell)$ by writing down a joint angular decay distribution involving the polar angles θ, θ_B and the azimuthal angles χ defined by the decay products in their respective CM (center of mass) systems as shown in Fig. 1.

3. The Transition Form Factors in the Covariant Confined Quark Model

We shall use the covariant confined quark model to describe the dynamics of the current–induced $\Lambda_b = (b[ud])$ to $\Lambda_c = (c[ud])$ transition (see Refs. 23 and 22). The starting point of the model is an interaction Lagrangian which describes the coupling of the Λ_Q-baryon to the relevant interpolating three-quark current. One has

$$\mathcal{L}_{\rm int}^{\Lambda_Q}(x) = g_{\Lambda_Q}\bar{\Lambda}_Q(x)\cdot J_{\Lambda_Q}(x) + g_{\Lambda_Q}\bar{J}_{\Lambda_Q}(x)\cdot\Lambda_Q(x),$$
$$J_{\Lambda_Q}(x) = \int dx_1\int dx_2\int dx_3 F_{\Lambda_Q}(x;x_1,x_2,x_3)J_{3q}^{(\Lambda_Q)}(x_1,x_2,x_3),$$
$$J_{3q}^{(\Lambda_Q)}(x_1,x_2,x_3) = \epsilon^{a_1a_2a_3}Q^{a_1}(x_1)u^{a_2}(x_2)C\gamma^5 d^{a_3}(x_3), \tag{8}$$
$$\bar{J}_{\Lambda_Q}(x) = \int dx_1\int dx_2\int dx_3 F_{\Lambda_Q}(x;x_1,x_2,x_3)\bar{J}_{3q}^{(\Lambda_Q)}(x_1,x_2,x_3),$$
$$\bar{J}_{3q}^{(\Lambda_Q)}(x_1,x_2,x_3) = \epsilon^{a_1a_2a_3}\bar{d}^{a_3}(x_3)\gamma^5 C\bar{u}^{a_2}(x_2)\cdot\bar{Q}^{a_1}(x_1).$$

The form factors describing the $\Lambda_Q \to \Lambda_{Q'}$ transition via the local weak quark current are calculated in terms of a two-loop Feynman diagram. Due to the confinement mechanism of the model, the Feynman diagrams do not contain branch points corresponding to on-shell quark production.

Table 1. q^2 averaged helicity structure functions in units of 10^{-15} GeV.

	Γ_U	Γ_L	Γ_{LT}	Γ_P	Γ_{Lp}	Γ_{LTp}
e	12.4	19.6	−7.73	−7.61	−18.5	−3.50
τ	3.29	2.90	−2.06	−1.73	−2.46	−0.66
	$\widetilde{\Gamma}_U$	$\widetilde{\Gamma}_L$	$\widetilde{\Gamma}_S$	$\widetilde{\Gamma}_{LT}$	$\widetilde{\Gamma}_{Sp}$	$\widetilde{\Gamma}_{SL}$
τ	0.66	0.63	0.64	−0.41	−0.55	0.55
	$\widetilde{\Gamma}_P$	$\widetilde{\Gamma}_{Lp}$	$\widetilde{\Gamma}_{LTp}$	$\widetilde{\Gamma}_{STp}$	$\widetilde{\Gamma}_{SLp}$	
τ	−0.37	−0.55	−0.14	−0.42	−0.64	

Table 2. The integrated quantities of physical observables.

	$\langle A_{FB}^{\ell} \rangle$	$\langle C_F \rangle$	$\langle P_z^h \rangle$	$\langle P_x^h \rangle$	$\langle P_z^{\ell} \rangle$	$\langle P_x^{\ell} \rangle$
$e^- \bar{\nu}_e$	0.18	−0.63	−0.82	0.40	−1.00	0.00
$\tau^- \bar{\nu}_\tau$	−0.038	−0.10	−0.72	0.22	−0.32	0.55

The results of our numerical two-loop calculation are well represented by a double–pole parametrization

$$F(q^2) = \frac{F(0)}{1 - as + bs^2}, \quad s = \frac{q^2}{M_1^2} \tag{9}$$

with high accuracy: the relative error is less than 1%.

In Table 1 we list q^2 averaged helicity structure functions in units of 10^{-15} GeV. The numbers in Table 1 show that the results of our dynamical calculation are very close to the HQET results $\widetilde{\Gamma}_L = \widetilde{\Gamma}_S = -\widetilde{\Gamma}_{SL_P}$, $\widetilde{\Gamma}_{S_P} = \widetilde{\Gamma}_{L_P} = -\widetilde{\Gamma}_{SL}$ and $\widetilde{\Gamma}_{ST_P} = \widetilde{\Gamma}_{LT}$. We do not display helicity flip results for the e mode, because they are of order 10^{-6}–10^{-7} in the above units.

In Table 2 we give the values of the integrated quantities. These can be obtained from the nonflip and flip rates collected in Table 1. In most of the shown cases, the mean values change considerably when going from the e to the τ modes including even a sign change in $\langle A_{FB}^{\ell} \rangle$.

Acknowledgments

We are grateful to the organizers for the invitation to the conference "Hadron Structure'15". This work was supported by the Tomsk State University Competitiveness Improvement Program and the Russian Federation program "Nauka" (Contract No. 0.1526.2015, 3854). M. A. I. acknowledges the support from the Mainz Institute for Theoretical Physics (MITP). M. A. I. and J. G. K. thank the Heisenberg-Landau Grant for support.

References

1. A. Soffer, *Mod. Phys. Lett. A* **29**, 1430007 (2014) [arXiv:1401.7947 [hep-ex]].

2. A. Celis, "$B \to D^{(*)}\tau\nu$ decays in the aligned two-Higgs-doublet model," arXiv:1410.1858 [hep-ph].
3. A. Crivellin, "Challenges for New Physics in the Flavour Sector," arXiv:1409.0922 [hep-ph].
4. T. Blake, T. Gershon and G. Hiller, *Ann. Rev. Nucl. Part. Sci.* **65**, 8007 (2015) [arXiv:1501.03309 [hep-ex]].
5. U. Nierste, S. Trine and S. Westhoff, *Phys. Rev. D* **78**, 015006 (2008) [arXiv:0801.4938 [hep-ph]].
6. A. Pich and P. Tuzon, *Phys. Rev. D* **80**, 091702 (2009) [arXiv:0908.1554 [hep-ph]].
7. M. Jung, A. Pich and P. Tuzon, *JHEP* **1011**, 003 (2010) [arXiv:1006.0470 [hep-ph]].
8. S. Faller, T. Mannel and S. Turczyk, *Phys. Rev. D* **84**, 014022 (2011) [arXiv:1105.3679 [hep-ph]].
9. A. Celis, M. Jung, X. Q. Li and A. Pich, *JHEP* **1301**, 054 (2013) [arXiv:1210.8443 [hep-ph]].
10. S. Fajfer, J. F. Kamenik, I. Nisandzic and J. Zupan, *Phys. Rev. Lett.* **109**, 161801 (2012) [arXiv:1206.1872 [hep-ph]].
11. S. Fajfer, J. F. Kamenik and I. Nisandzic, *Phys. Rev. D* **85**, 094025 (2012) [arXiv:1203.2654 [hep-ph]].
12. A. Datta, M. Duraisamy and D. Ghosh, *Phys. Rev. D* **86**, 034027 (2012) [arXiv:1206.3760 [hep-ph]].
13. A. Crivellin, C. Greub and A. Kokulu, *Phys. Rev. D* **86**, 054014 (2012) [arXiv:1206.2634 [hep-ph]].
14. X. G. He and G. Valencia, *Phys. Rev. D* **87**, 014014 (2013) [arXiv:1211.0348 [hep-ph]].
15. M. Tanaka and R. Watanabe, *Phys. Rev. D* **87**, 034028 (2013) [arXiv:1212.1878 [hep-ph]].
16. P. Biancofiore, P. Colangelo and F. De Fazio, *Phys. Rev. D* **87**, 074010 (2013) [arXiv:1302.1042 [hep-ph]].
17. M. Duraisamy, P. Sharma and A. Datta, *Phys. Rev. D* **90**, 074013 (2014) [arXiv:1405.3719 [hep-ph]].
18. J. G. Körner and G. A. Schuler, *Z. Phys. C* **38**, 511 (1988) [Erratum-ibid. C **41**, 690 (1989)].
19. J. G. Körner and G. A. Schuler, *Phys. Lett. B* **231**, 306 (1989).
20. J. G. Körner and G. A. Schuler, *Z. Phys. C* **46**, 93 (1990).
21. T. Gutsche, M. A. Ivanov, J. G. Körner, V. E. Lyubovitskij, P. Santorelli and N. Habyl, *Phys. Rev. D* **91**, 7, 074001 (2015) [*Phys. Rev. D* **91**, 11, 119907 (2015)] [arXiv:1502.04864 [hep-ph]].
22. T. Gutsche, M. A. Ivanov, J. G. Körner, V. E. Lyubovitskij and P. Santorelli, *Phys. Rev. D* **88**, 11, 114018 (2013) [arXiv:1309.7879 [hep-ph]].
23. T. Gutsche, M. A. Ivanov, J. G. Körner, V. E. Lyubovitskij and P. Santorelli, *Phys. Rev. D* **87**, 074031 (2013) [arXiv:1301.3737 [hep-ph]].